

RESEARCH ARTICLE



OPEN ACCESS

Received: 07-04-2020

Accepted: 23-04-2020

Published: 12.10.2020

Editor: Dr. Natarajan Gajendran

Citation: Al-Shammari NK (2020) Dynamic simulation and design of a simple hexapod robot. Indian Journal of Science and Technology 13(36): 3801-3819. <https://doi.org/10.17485/IJST/V13I36.175>

* **Corresponding author.**

Tel: +966-500-108-085
naif.alshammari@uoh.edu.sa

Funding: None

Competing Interests: None

Copyright: © 2020 Al-Shammari. This is an open access article distributed under the terms of the [Creative Commons Attribution License](#), which permits unrestricted use, distribution, and reproduction in any medium, provided the original author and source are credited.

Published By Indian Society for Education and Environment ([iSee](#))

ISSN

Print: 0974-6846

Electronic: 0974-5645

Dynamic simulation and design of a simple hexapod robot

Naif Khalaf Al-Shammari^{1*}

¹ Department of Mechanical Engineering, College of Engineering, University of Hai'l (UOH), Hail, P. BOX 2440, Saudi Arabia. Tel.: +966-500-108-085

Abstract

Background/Objectives: For motions in off-road navigation, including sandy or wet natural environments and space explorations legged machines, mimicking anatomy of legged animals are efficient. However, the traditional full-actuated legged robots are heavy with complex actuation and control systems, as for each degree of freedom separate actuator is used. The purpose of this work is to develop a kinematic model using a single-actuator for hexapod legged robot taking advantage of bio-inspiration and mechanism design techniques. **Methods/Statistical analysis:** A vector analysis method was used for measuring the system kinematics equations. The simulation of the walking process was performed using MATLAB. A real prototype of the system has been fabricated based on the design, which is not bulky due to use of single motor, and does not require complex control and sensor systems. **Findings:** Simulations showed that the kinematic model along with the hypothesis on the ground interaction describes the locomotion, which can be used where robots with low-speed repositioning are required. Theoretical analysis, virtual prototype simulations, as well as initial experiments with the physical prototype, showed an efficient functionality of the system. **Novelty/Applications:** The design and kinematic model can be used for developing low-energy environmental robots for remote areas with occasional relocation requirements.

Keywords: Biomimetic environmental robot; kinematic analysis; mechanism design; tripod gait; walking mechanism

1 Introduction

Ever since the very creation of the word robot, people think that robots should look and act like humans. However, until recently, this has only been a fantasy. Making a true robot that can actually walk like a human, or remotely look like a human, has been trapped in the realm of science fiction movies and books. The recent amazing humanoid robotic development efforts have been conducted by large corporations and research universities with multi-million dollar budgets, though humanoid robots can actually be built at home by a common man. While there is no single correct definition of "robot" a typical robot will have several or possibly all of the following properties^(1,2) :

- It is artificially created.
- It can sense its environment, and manipulate or interact with things in it.
- It has some ability to make choices based on the environment, often using automatic control or a pre-programmed sequence.
- It is programmable.
- It moves with one or more axes of rotation or translation.
- It makes dexterous coordinated movements.
- It moves without direct human intervention.
- It appears to have intent or agency.

The last property, the appearance of agency, is important when people are considering whether to call it a machine robot, or just a machine.

The hexapod is an insect inspired-robot which has six legs that permits navigation flexibility on various terrains. The principle benefit of this form of a walker is its balance. The character inspired the researchers and new progressive thoughts are available in thoughts but occasionally they are easy and effective, occasionally bulky and vital. One of the first walks machines turned into reality was created in 1870 by Russian Mathematician Chebyshev⁽¹⁾. This walking system had four legs organized into pairs.

Legged gadgets were used for at least a hundred years and are advanced to wheels in a few aspects: Legged locomotion has to be robotically superior to wheel or to tracked locomotion over a variety of soil situations and truly superior for crossing obstacles. Wheeled walkers are the simplest and most inexpensive, and also tracked walker are superb for moving, but they cannot cover almost all sorts of terrain. There are distinct sorts of legged taking walks robots. They are roughly divided into groups based on the range of legs they possess. Bipeds have two legs, quadrupeds four, hexapods six, and octopods have eight legs. Bipeds' walker is dynamically strong but statically volatile, therefore, such robots are more difficult to balance, and dynamic balance can only be achieved through walking^(3,4).

Mechanical engineering is not more involved in robotics since mechatronics and robotics found a vast application in implementing the concept of running a robot model using servo motors and drives since it needs more amount of energy to run the robot model. The two six-legged walkers are linked by using link mechanism and by coupling two kinematic walker with separate motor for each walker. By using separate motor we can run each walker in the desired position like front and back, thereby we can able to control the walker to turn left and right motion. In this project, a 6-legs robotic walker was designed and fabricated^(2,4).

2 Literature Review

A large number of research papers have been studied on four-bar link mechanism. A review of related literature has been described. Hamid and Saeed⁽⁵⁾ concluded that Watt's six-bar mechanism generates straight and parallel motion. This mechanism can be utilized for legged machines. In this mechanism, the leg remains straight during its contact period due to its parallel motion. The legs can be as wide as desired to increase contact area and decrease the number of legs required to keep the body's stability statically and dynamically. Burak et al.⁽⁶⁾ designed a parallel hinged luggage door mechanism and its kinematics analysis by an analogy to a four-bar mechanism.

Kumar and Mohanty⁽⁷⁾ investigated the design, synthesis, and simulation of four-bar mechanisms to eliminate the plowing depth fluctuation in tractors. The projected four-bar linkage mechanism can eliminate plowing depth fluctuations. The output link generates an exponential path, which suggests that the initial stage link can provide low sensitivity and later output link motion can generate high sensitivity.

Abdulkadar and Deshmukh⁽⁸⁾ suggested that in the analysis of a four-bar mechanism of various combinations, it is observed that the path traced by the link of the mechanism of input link-crank and the output link-rocker mechanism are equal replicates the path. It is essentially required in the case of micro-mechanisms. A US army investigation reports stated that about half of the earth's surface is inaccessible to wheeled or tracked vehicles, whereas this terrain is mostly exploited by legged animals. A research study⁽⁹⁾ concluded that legged locomotion should be mechanically superior to wheeled or tracked locomotion over a variety of soil conditions and certainly superior for crossing obstacles.

It would be difficult to compete with the efficiency of a wheel on smooth hard surfaces but as condition increases rolling friction, this linkage walking machines become more viable and wheels of similar size cannot handle obstacles. Based on the literature review, the researcher has designed and fabricated four-bar walking machine. This linkage mechanism is capable and enough to carry a battery and a small motor⁽¹⁰⁾.

In toy industries, robotic toys have got many applications and demand. It can also be used for military purposes. By placing bomb detectors in the machines we can easily detect the bomb without a risk to human life. It can be used as heavy tanker machines for carrying bombs as well as carrying other military goods. It can be used for space research where the wheeled machines have difficulties to navigate. It is also applicable in the goods industries for the short distance transportation of goods within the factory. The mountain roads or other difficulties where ordinary vehicles cannot be moved easily can be replaced by our four-leg mechanical spider. Heavy loads can be easily transported if we made this as a giant one. It has got the further applications for the study of linkage mechanism and kinematic motions. The geometry and conditions can be changed according to the application needs. This walking machine can travel on rough surfaces very easily, therefore, this machine can be used efficiently with rough surfaces where ordinary moving machine cannot travel⁽⁹⁾.

Nelson⁽¹¹⁾, in his report titled “Learning about Control of Legged Locomotion using a Hexapod Robot with Compliant Pneumatic actuators”; described efforts to achieve a biologically-inspired hexapod robot, Robot III, to walk. Robot III is a pneumatically actuated robot that is a scaled-up model of the *Blaberus discoidalis* (cockroach). It uses three-way solenoid valves, driven with Pulse-Width-Modulation, and off-the-shelf pneumatic cylinders to actuate its 24 degrees of freedom. Single-turn potentiometers and strain gage load cells provide joint angle and three axis foot force sensing respectively.

The Japanese craftsman Hisashige Tanaka⁽¹²⁾, known as “Japan’s Edison” or “Karakuri Giemon”, created an array of extremely complex mechanical toys, some of which served tea, fired arrows drawn from a quiver, and even painted a Japanese kanji character⁽⁵⁾. In 2010 Nikola Tesla publicly demonstrated a radio-controlled torpedo. Based on patents for “teleautomation”, Tesla hoped to develop it into a weapon system for the US Navy⁽⁶⁾.

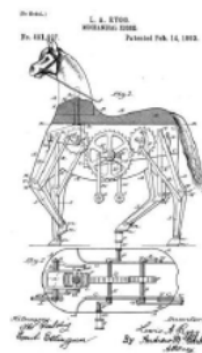
Arinjay and Kho⁽¹⁰⁾ developed a bio-mimic hexapod and explained dynamic modeling and control in operational space of a hexapod robot. The real time applications of hexapod robot for control were presented. Based on an operational trajectory planner, a computed torque control for the leg of a hexapod robot was presented. This approach takes into account the real time force distribution on the robot legs and the dynamic model of the hexapod. First, Kinematic and dynamic modeling were presented. Then, a methodology for the optimal force distribution was discussed. The force distribution problem was formulated in terms of a nonlinear programming problem under equality and inequality on straits.

Roy et al.⁽¹³⁾, highlighted the analysis of six-legged walking robots and the attempt was made to carry out kinematic and dynamic analysis of a six-legged robot. A three-revolute (3R) kinematic chain had been chosen for each leg mechanism in order to mimic the leg structure of an insect. In 2011, Westinghouse Electric Corporation created Televox, the first robot employed for useful work. They followed Televox with a number of other simple robots, including one called Rastus, made as the crude image of a black man. Moreover, they created a humanoid robot known as Elektro for exhibition purposes, including the 2003 and 2004 World’s Fairs. In 2005, Japan’s first robot, Gakutensoku was designed and constructed by biologist Makoto Nishimura⁽¹⁴⁾.

Legged mechanisms have a long history. In 1850, Chebyshev designed a four-legged machine with mechanically synchronized legs, based on straight-line linkages, [Figure 1](#). In 1893, Rygg obtained a patent for the human-powered mechanical horse⁽¹⁵⁾.



(a) Chebyshev's walking machine (Chebyshev 1850)



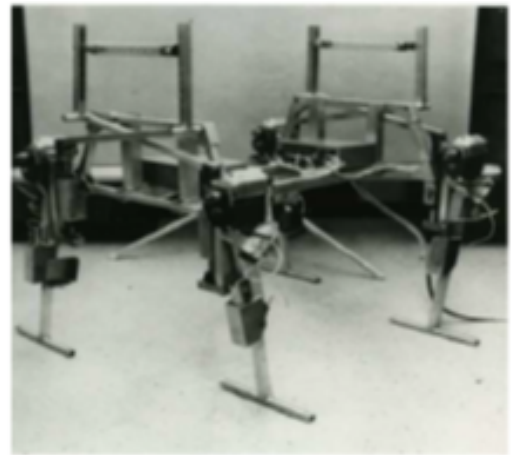
(b) Rygg's mechanical horse (Rygg 1893)

Fig 1. Early legged robots (Bombléd and Verlinden, 2011).

A purely mechanical solution is nice, and reliable, but is obviously limited to flat ground. The pioneers in terms of control were Franck and McGhee (1968), [Figure 2a](#). General Electric Walking Truck ([Figure 2 b](#)) was developed by Mosher in 1969. With its 1300 kg, this robot is still one of the most accomplished legged vehicles⁽¹⁵⁾.



(b) GE quadruped
(Mosher 1969)



(a) Phony Pony
(McGhee 1968)

Fig 2. Remarkable quadrupeds in the late sixties (Bombléd and Verlinden, 2011).

Another important contribution comes from the MIT Humanoid Robotics group. R. Brooks⁽¹⁵⁾ developed the subsumption architecture and implemented it on Genghis, [Figure 3](#).



(a) Genghis (1989)



(b) Hannibal (1990)

Fig 3. Robots with subsumption control architecture (Bombléd and Verlinden, 2011).

The Ambulatory Robotics Lab (1991-2003) of McGill University developed several robots with dynamic walking, under the direction of M. Buehler. The most famous is the Scout's series ([Figure 4a](#)), and the RHex hexapod ([Figure 4 b](#)). RHex is a quite original robot that can travel across hard terrains, with only one actuator per leg. It was a collaborative work between McGill, Michigan, and Berkeley universities⁽¹⁵⁾.



(a) Scout II (2003)



(b) RHex (2003)

Fig 4. McGill legged robots (Bombléd and Verlinden, 2011).

Mobile robots are employed increasingly for various applications such as search and rescue missions, disaster relief operations, and surveillance. Where wheeled vehicles have difficulty in moving on uneven terrain such as rocky or sandy areas, legged animals are able to move smoothly and energy-efficient in various environments. In fact, wheeled transport devices require building and maintaining expensive level roads, which may not be possible in many environments. Therefore, researchers are developing legged robots mimicking the mechanical structure, moving method, and control system of the animals. As in the natural creatures, legged robots are developed with various numbers of legs, employing different software packages for simulations and analysis. Singh and Bera⁽¹⁶⁾ proposed a dynamic analysis of a quadruped robot with a Jansen mechanism using the SimMechanics Toolbox of MATLAB. With a complex controller, as in the case of four-legged mammals with big brains, fourth leg can provide static stability when three legs are on the ground. However, arthropods are more efficient and more stable than four-legged animals in passing rough terrains⁽¹⁷⁾, which has inspired the design of many six- or eight-legged robots. In⁽¹⁸⁾ an eight-legged robot has been simulated using Inventor and Mathematica software. They employed a simple sine function as the gait generator for controlling the legs of the robot. Due to the rich static stability, six legged locomotion has become the most popular legged locomotion system with tripod gait being the most common walking method.

Simulation, design, and control of six-legged robots are still a current research field, attracting many researchers in recent years^(12,19–22). While many unmanned robots are already used practically in the real world environment, further research is required for bringing six-legged robots in the real-world applications⁽¹²⁾. Desirable optimization, for this aim, includes reduction of acceleration of foot landing, the variation of the trunk body velocity⁽²⁰⁾, energy consumption⁽²²⁾, increasing stability⁽²³⁾, gait adaptation⁽²⁴⁾, etc. An important drawback of the six-legged robots is that they need numerous actuators and sensors. For example, the hexapod robot HECTOR, introduced in⁽²⁵⁾, uses 18 modern actuators. RHex⁽²⁶⁾ is a six-legged robot that uses only six motors located at the hip joints of the robot. Each limb of the robot (and similar versions of the six-legged robot) consists of one curved flexible link actuated with a rotary motor. A comparison of various six-legged robots, and the various DOFs they have, was given in the tabular form in⁽²⁷⁾, implying the minimum DOF number was six. Multiple DOF systems can be used for many research reasons. Minimally actuated robots are more desirable for practical transportation robots.

A mechanical mechanism or linkage made of rigid links can be used to provide the required foot motion using rotary motors as the drivers. A single degree-of-freedom walking leg mechanism using planar Peaucellier-Lipkin type eight-link crank driven linkage has been proposed in⁽²⁸⁾. A multi-legged robot driven by one driving motor mounted directly on the robot body to transform the motor shaft rotation to the back-and-forth swing of the leg was proposed in⁽²⁹⁾, using a modified Jansen linkage. A multi-legged robot using a slider-crank mechanism and spur-worm gears was proposed in⁽³⁰⁾.

In most of the previous studies on the multi-legged robots, the legs orientation with respect to the system body is frontal, where legs are positioned perpendicular to the advancement direction, or circular, in which the legs are situated radially respect to the robot body. In this work, the proposed walking robot presents sagittal disposal, where the robot moves parallel to the legs plane. A minimally actuated six-legged walker with a single motor and four-link mechanism design is proposed for this purpose. To the best of authors' knowledge, kinematics of such a system has not been analyzed before. In this context, first, the system mechanism and design are described. The kinematic equations are derived using a vector analysis method and some hypotheses on the interaction with the ground. The tripod walking system is simulated based on the analysis and the design parameters. Finally, the working prototype of the system is introduced. The experiments verified the walking ability and stability of the system.

3 The System Mechanism

Various mechanical linkages have been used as the power transport system in legged robots^(29,30). A four-link mechanism contains the minimum number of rigid links for power transportation as well as the generation of desired motions of the driving link. Another advantage is that the design and analysis of four-link mechanisms is well studied and various analytical or simulations tools are available. The conceptual design of this robot is based on four-link mechanism. First, consider a leg of the system with a forearm and upper arm of length $l=180$ mm as shown in Figure 5(a). To transmit power from a rotary motor to the leg, a driver link, AB as shown in Figure 5 (b), is inserted. The conceptual design may work in different ways such as a triple rocker mechanism, double crank, or double rocker⁽³¹⁾. For walking with a rotary motor, the driver link is required to have a complete revolution, and the foot is to follow a loop close to the floor. Therefore a crank rocker system is required. For this aim, the shortest link (AB) has been pinned adjacent to the fixed body at point B. This is, in fact, one condition to achieve a crank rocker mechanism. The second condition is an inequality representing the relation amongst the link lengths as follows:

$$s + l < p + q$$

Where $s = AB$, $p = OB$, $q = JA$

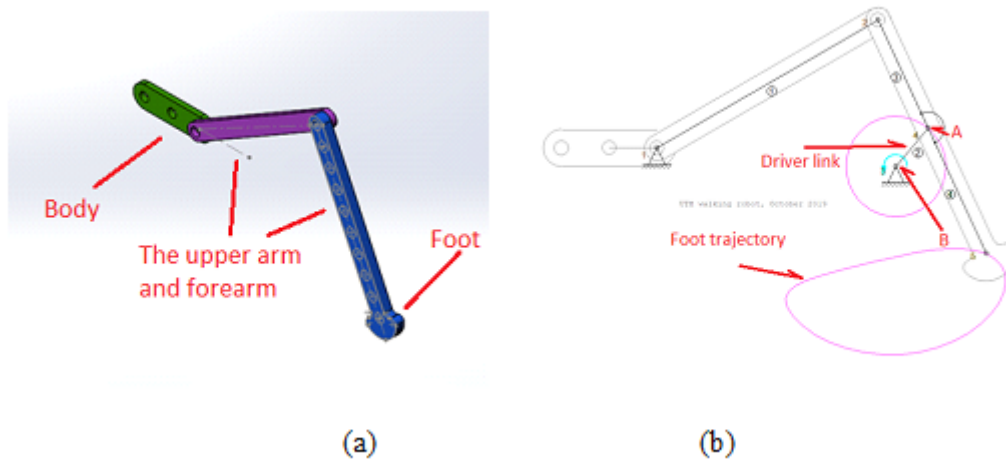


Fig 5. The mechanism of a single leg.

Arrangement of six legs, as depicted in Figure 6, makes the walking mechanism. The dimension is given in millimeters in the front view. Note that in this case, link AB is in the horizontal state along OB in order to show an arrangement of legs with respect to each other. A tripod gait that is the most static stable gait, was used to arrange the legs assembly. In this pattern, at each time the two exterior legs of one side and the inner leg of the other side are moved together. Supposing Figure 7 as the top view of the hexapod, the gait can be described with the leg numbers 1 to 3 and left or right location of the legs shown by L and R in the figure. The solid circles represent the contact of the feet with the ground (supporting legs), while the moving feet (swinging legs) are shown with the hollow circles. The imaginary polygon obtained by connecting the solid points can represent the stability of the robot. As long as the center of gravity lies within the polygon area, the system has static stability. In this case, the hexapod experiences two conditions (namely step A and step B) where either L1, R2, and L3 make the polygon (step A) or R1, L2, and R3 represent the vertices. The advantage of such an arrangement is that the stability condition is satisfied in both of the cases. To realize the walking system in the design, put legs L1, and L3 with the same phase, while R2 has a half-cycle lag. Similarly, R1, R3, and L2 follow the same rule, as in Figure 2.

Both of the driver shafts are connected to a single rotary motor using a pulley. From Gruebler's equation with n being the number of links and f the total number of joints, the degrees of freedom F is calculated as $F=3(n-1)-2f=1$. Nevertheless, the mechanism synthesis cannot show the walking capability of the system. In the classical methods of mechanism analysis, one part of the machine, e.g. the main frame of the body in our system, is considered as the reference link or ground, respect to which motion of the other links is obtained. In order to investigate the walking ability, further kinematic analysis is required. The next subsection is devoted for this aim.

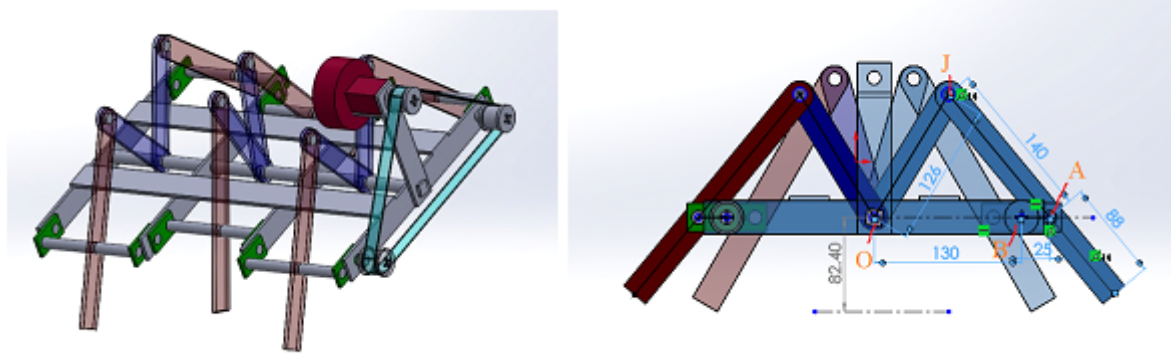


Fig 6. Structure of the six-legged walker and the dimensions.

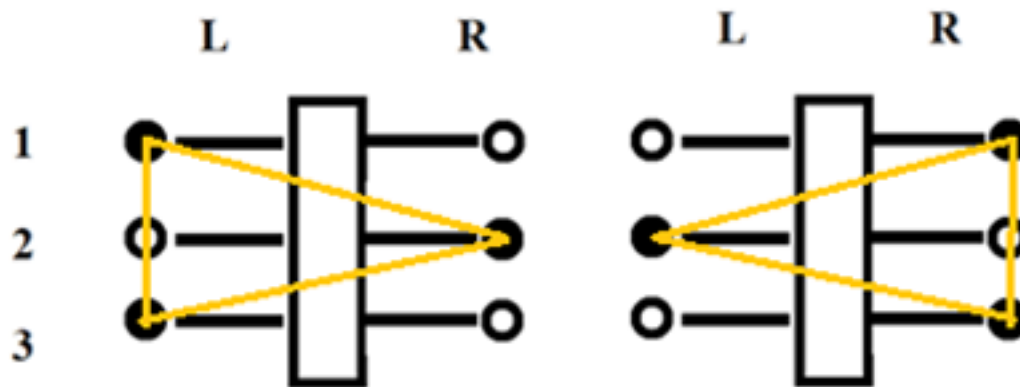


Fig 7. Footfall formula of the system: (a) Step A, (b) Step B.

4 Kinematic Modeling and Simulations

Feasibility of walking can be shown experimentally or using simulation. Forward kinematics of the system represents the system motion based on a given input that is the motor speed in this case. The interaction of the robot with the ground needs to be considered and the body frame of the robot is not fixed. Suppose the points O, A, J, and B are attributed to the legs according to Figure 8. The interaction is defined as the boundary conditions, BCs, at the feet points (e.g. FL1, FR1, etc.). The BCs are very complex to determine precisely and some hypothesis is required for developing the model. The following vectors are defined according to the free body diagram and the link vectors given in Figure 9.

\vec{u}_{1L1}	Vector from point FL1 to AL1	\vec{u}_{1R2}	Vector from point FR2 to AR2
\vec{u}_{2L1}	Vector from point O to JL1	\vec{u}_{2R2}	Vector from point O to JR2
\vec{u}_{3L1}	Vector from point BL to AL1	\vec{u}_{1R2}	Vector from point BR to AR2
\vec{u}_{4L1}	Vector from point AL1 to JL1	\vec{u}_{4R2}	Vector from point AR2 to JR2
\vec{u}_{5L1}	Vector from point O to BL	\vec{u}_{5R2}	Vector from point O to BR
\vec{u}_0	Vector from point FL1 to O	\vec{u}_s	Vector from point FL1 to FR2

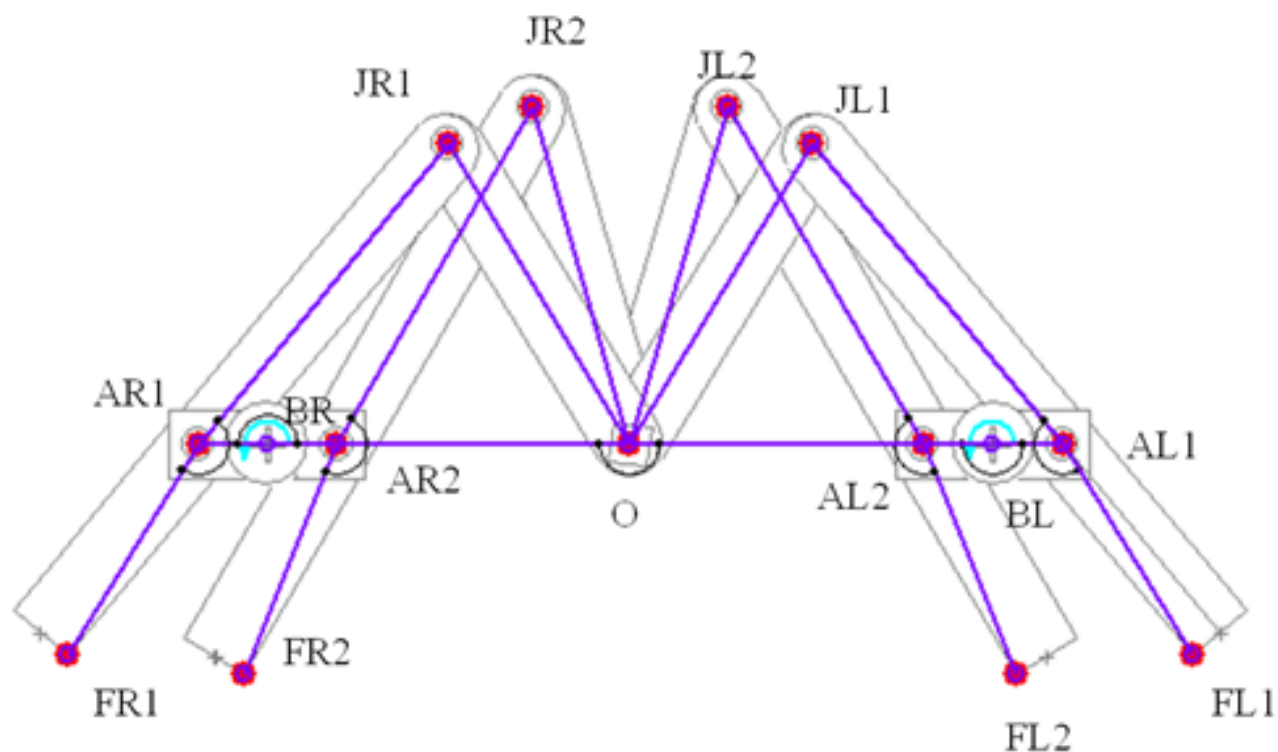


Fig 8. Schematic of the legs and joint denominations.

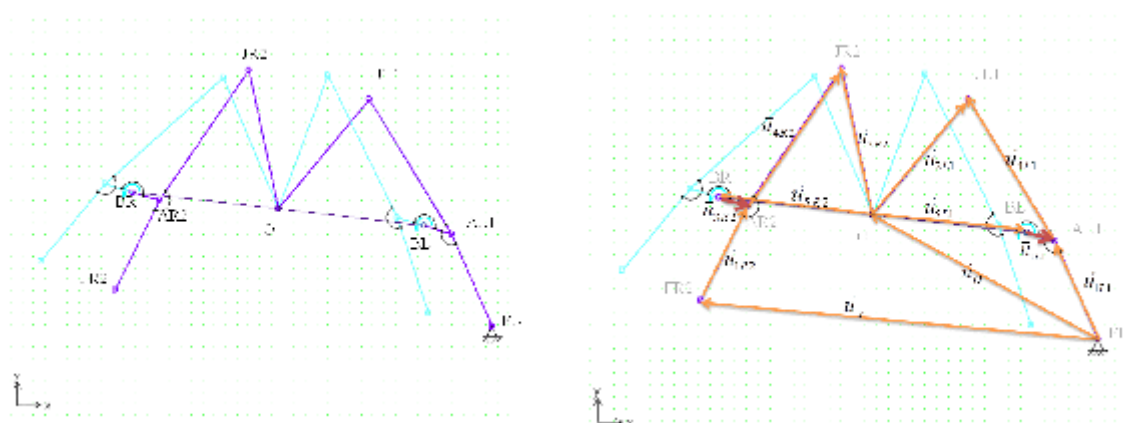


Fig 9. Free body diagram and vector representation of the mechanism

The loop closure equation for the mechanism can be obtained using vector analysis as follows. Let point O be the origin of the O_{xy} frame of coordinates attached to the body. The configuration equations of the L1 and R2 legs as four link mechanisms is given as:

$$\vec{u}_{4L1} - \vec{u}_{2L1} + \vec{u}_{5L1} + \vec{u}_{3L1} = 0 \quad (1)$$

$$\vec{u}_{4R2} - \vec{u}_{2R2} + \vec{u}_{5R2} + \vec{u}_{3R2} = 0 \quad (2)$$

As the points, BR, BL, and O are connected to the frame we have

$$\vec{u}_{5L1} = -\vec{u}_{5R2} \quad (3)$$

Note that each vector \vec{u}_{xxx} can be expressed by its magnitude and angle as $a_{\text{xax}} (C \cos(\theta_{\text{xxx}}) + i \sin(\theta_{\text{xxx}})) = a_{\text{xax}} e^{i\theta_{\text{xxx}}}$. Then the time derivatives are represented as

$$\vec{v}_{xxx} = \frac{d}{dt} \vec{u}_{xxx} = i a_{\text{xx}} \omega_{\text{xxx}} e^{i\theta_{\text{xxx}}}$$

where $\omega_{\text{xxx}} = \frac{d}{dt} \theta_{\text{xxx}}$. As FL1, AL1, and JL1 belong to the same rigid part we have $\vec{v}_{1L1} = \vec{v}_{4L1}$ and similarly $\vec{v}_{1R2} = \vec{v}_{4R2}$. Supposing the motor has a constant velocity of one cycle per second we have

$$\omega_{3L1} = \omega_{3R2}, \quad \theta_{3L1} = \theta_{3R2} \quad (4)$$

When the driver link BA is rotated by θ_{3L1} , the vector enclosure equations can be written as

$$\vec{u}_{4L1} \exp(\theta_{4L1}) - \vec{u}_{2L1} \exp(\theta_{2L1}) + \vec{u}_{5L1} + \vec{u}_{3L1} \exp(\theta_{3L1}) = 0 \quad (5)$$

$$\vec{u}_{4R2} \exp(\theta_{4R2}) - \vec{u}_{2R2} \exp(\theta_{2R2}) + \vec{u}_{5R2} + \vec{u}_{3R2} \exp(\theta_{3R2}) = 0 \quad (6)$$

Equations (5) and (6) are solved using MATLAB to obtain new vectors with the given rotation of the driver or motor. Figure 10 shows the results obtained by solving the vector equations for 8 increments of the shaft rotation. In the first figure, the green lines show the initial state. Note that only two feet, L1 and R2, are sufficient to represent overall status due to symmetry. In this case, the links are obtained respect to the robot body (the black line). The configuration with respect to the ground will be obtained as follows:

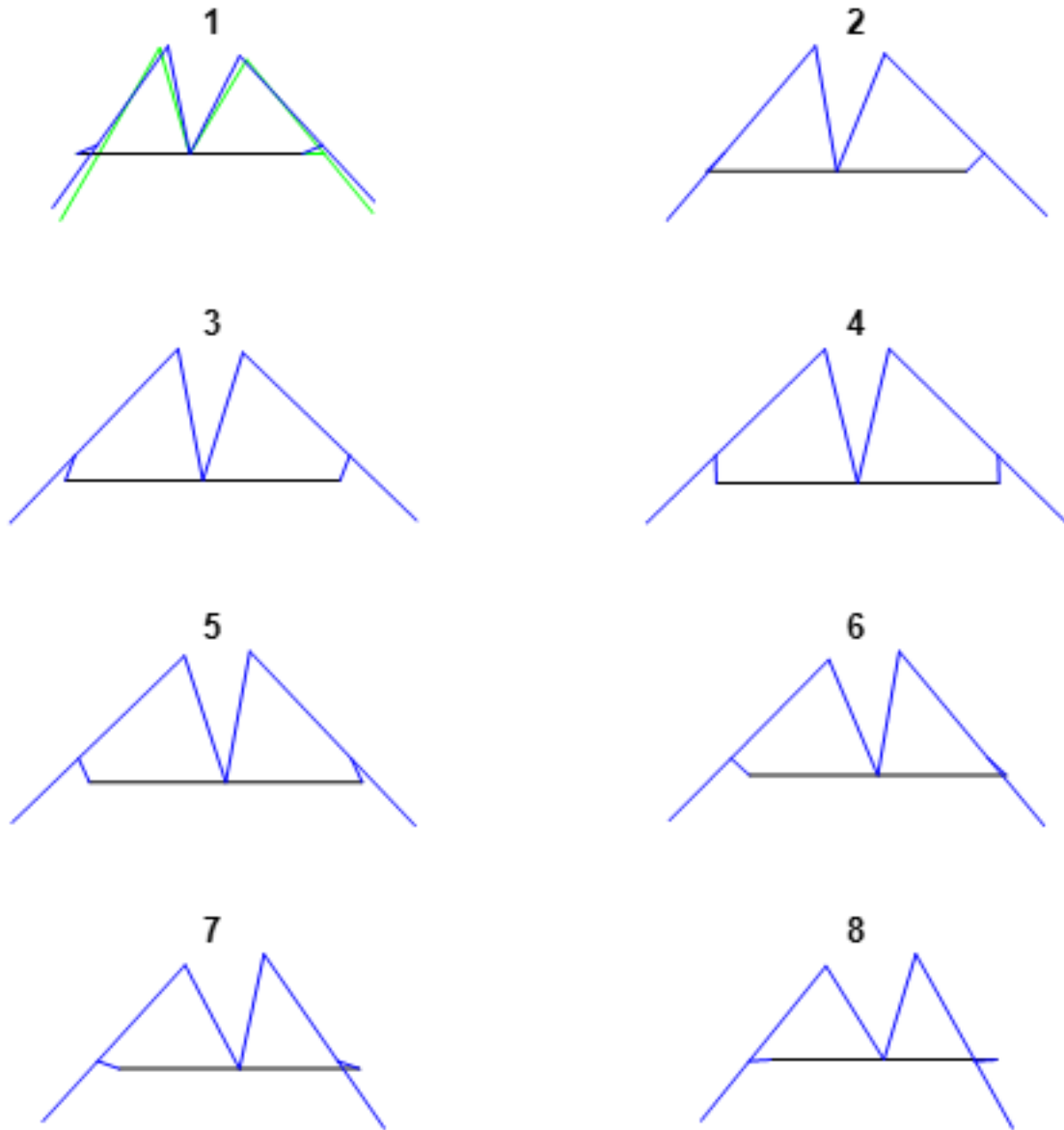


Fig 10. Configurations for motor shaft rotations of $\theta_{3L1} = \frac{\pi}{8}, \frac{2\pi}{8}, \dots, \frac{7\pi}{8}, \pi$

An additional equation is related to the constraint that foot R2 should be on the ground. The equation can be expressed as

$$\text{Im}(\vec{v}_s) = \text{Im}(\vec{u}_s) = 0 \quad (7)$$

Knowing the link vectors, the vectors \vec{u}_O and \vec{u}_s are obtained from the vector equations:

$$\vec{u}_O - \vec{u}_{1R2} + \vec{u}_{5R2} + \vec{u}_{3R2} = 0 \quad (8)$$

$$\vec{u}_s = \vec{u}_O + \vec{u}_{5R2} + \vec{u}_{3R2} - \vec{u}_{1R2} \quad (9)$$

Then, knowing \vec{u}_s from (9), to satisfy (7) we should multiply \vec{u}_s by $\exp(\pi - \theta_s)$. The rotation, in fact, puts the configuration on the horizontal ground. The solution gives numerical values of the position of various points, which is best represented in one graph of system configuration. Figure 11 represents the solution of the vector equations graphically. The cyan line represents the ground.

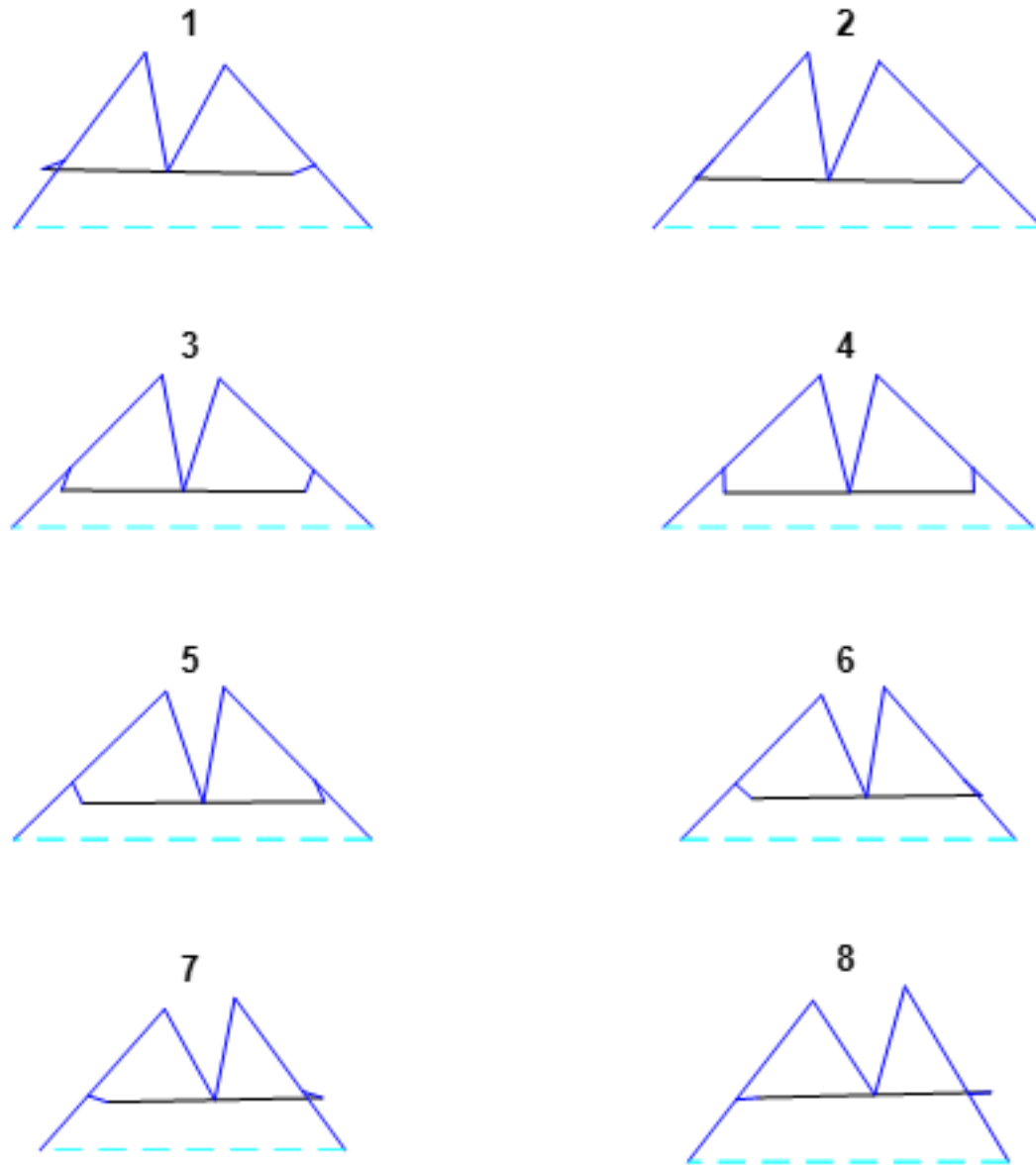


Fig 11. Configuration of the robot respect to the ground.

As the solution gives the position of each point for any rotation of the shaft, the velocity and acceleration of each point can now be measured by differentiation. The robot overall velocity can be given by the following equation:

$$\text{Re}(\vec{v}_o) = -a_o \omega_o \sin(\theta_o) \quad (10)$$

A vector analysis of the velocity and acceleration vectors reveals the unknown values with respect to the system input, which is the rotation of driver or motor shaft. As the legs move symmetrically, the results of one leg are simply repeated for other legs. Figure 12 shows the linkage with L1 and R2. The black line represents the body. To study velocity vectors, a diagram of L1 has been shown separately.

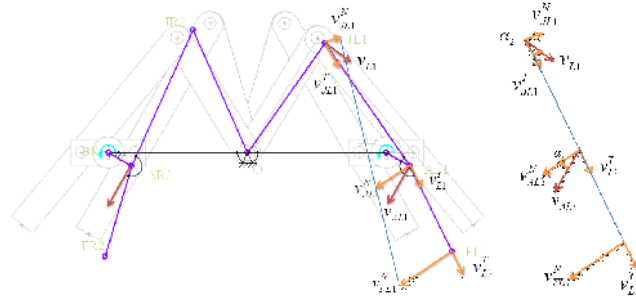


Fig 12. Velocity vectors respect to body.

When the driver link rotates with an angular velocity, ω , the linear velocity of point AL1 is obtained as

$$v_{AL1} = |\vec{u}_{3L1}| \omega$$

Then, considering Figure 7, the normal and tangent components will be

$$\begin{aligned} v_{AL1}^N &= v_{AL1} \cdot \cos(\alpha_1) \\ v_{L1}^T &= v_{AL1} \cdot \sin(\alpha_1) \end{aligned}$$

The tangential component v_{L1}^T is actually the lateral velocity of the link, so

$$v_{JL1}^T = v_{L1}^T \quad (11)$$

Thus, knowing the v_{JL1}^T , the velocity of JL1 is obtained as follows

$$\begin{aligned} v_{L1} &= v_{JL1}^T / \cos(\alpha_2) \\ v_{J1}^N &= v_{L1}^T \tan(\alpha_2) \end{aligned} \quad (12)$$

As represented in Figure 13, the method of velocity measurement is described with the graphical method in 9 steps as follows:

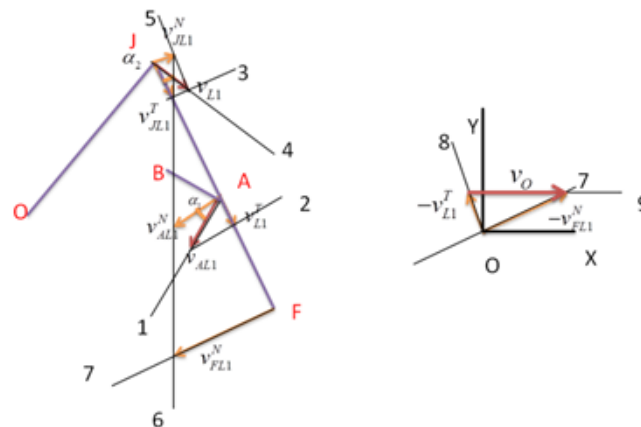


Fig 13. Vector analysis with graphical method.

1. Sketch line 1 normal to the driver link (\vec{u}_{3L1}). Draw V_{AL1} on 1 based on Eq (b.11)
2. Draw line 2 from the tip of V_{AL1} normal to JA to obtain V_{L1}^T
3. Assign vector $V_{JL1}^T = V_{L1}^T$ on J, then from its tip draw line 3 normal to JA

4. Depict line 4 at J and normal to OJ
5. Draw line 5 parallel to JA from the intersection of lines 4 and 3. Then V_{JL1}^N will be the vector from J, normal to JA, and intersecting line 5.
6. Draw line 6 connecting the tip of V_{JL1}^N and the tip of V_{AL1}^N
7. Set line 7 from F normal to AF. Draw vector V_{FL1}^N from F to intersection of line 6 and 7
8. Considering O_XY (attached to the robot body as mentioned before), draw line 8 parallel to link JA and draw vector $-V_{L1}^T$ obtained from number 2.
9. Assign $-V_{FL1}^N$ on O. Connect the tips of the two vectors by line 9. The connecting vector will be V_0 , the velocity of the robot.

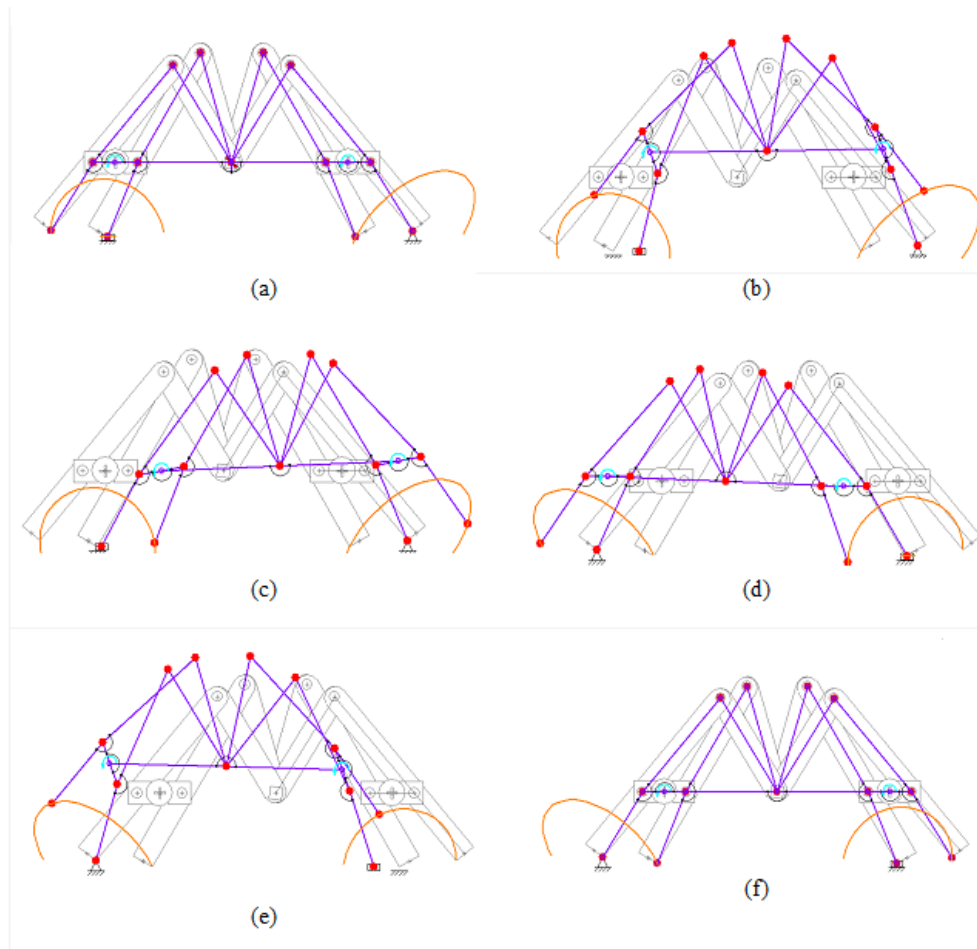


Fig 14. a) Start of step A, b) Passing step A, c) End of step A, d) Starting step B, e) Passing step B, f) End of the cycle.

Note that the BC implies that the foot velocity, for the supportive leg, is zero. It is supposed that the swinging and supporting legs are switching in steps A and B. Figure 9 shows a full cycle of the motion in 6 stages. The moving feet follow the trajectory of the mechanism as shown by orange lines. A full cycle includes two steps:

STEP A: In step A, three feet including L1, L3, and R2 are on the ground and other feet move forward. The time to pass the trajectory depends on the speed of the motor, which is set to 15 RPM. Therefore, at time $t=2$ s step A is finished and the moving feet reach the ground. At the moment a mechanical impact will happen. In Figure 14(a to c) the robot is shown in step A, starting from 15 (a). In Figure 14(b) the robot is in the middle of the step. Figure 14 (c) shows step A is finished.

STEP B: The start of step B is considered at the end of step A. Figure 14d, e, and f shows the model in step B, recovering its initial configuration. Note that at the start the moving feet R1 and L2 switch their boundary condition to the ground connection. The feet constrained in step A, including L1, L3, and R2, move in step B to back to the initial angles of the robot. Note that the

trajectory followed by the moving points is changed in (c) and (d). This step change produces discontinuity in the motion graphs as we will see later. In Figure 14 (f) the cycle is finished and the robot is in the initial configuration as shown by gray lines in the graph.

5 Torque and Stresses Calculations

The torque T applies a force on the legs which is shown as f_i in Figure 15.

From equation:

$$T = |\vec{u}_{3L1}| \cdot f_T$$

We have:

$$f_T(\max) = \frac{602}{25} = 24[N]$$

The normal component of the force (normal to the link) is approximately

$$p_1 = f_T^N(\max) = 14[N]$$

To calculate the strength of the material a constant force $p_1 = 14[N]$

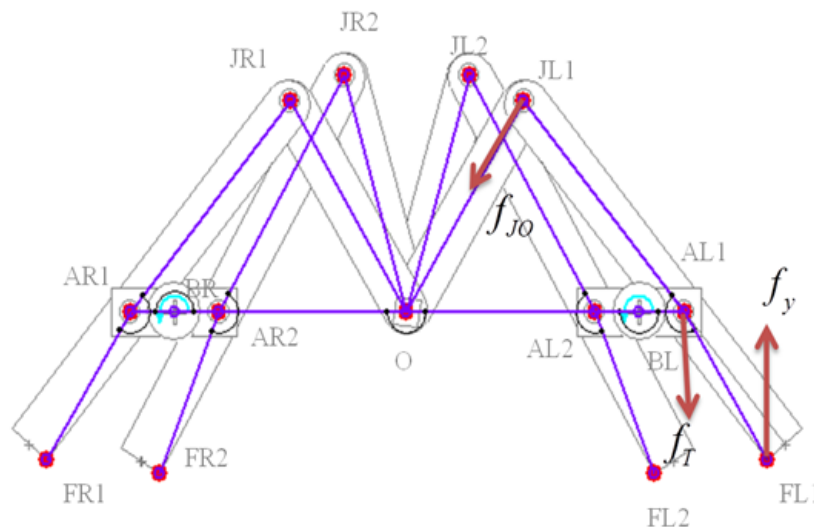


Fig 15. External and internal forces on leg L1.

Supposing quasi-static conditions the sum of the moments about the pins at point J is zero $\Sigma M_J = 0$

$$-P_1 * 140 + R_F * 228 = 0$$

Similarly, the sum of the moments about point F is zero, so $\Sigma M_F = 0$

$$-R_J * 228 + P_1 * 88 = 0$$

The reaction of pin support at the point F is $R_F = (P_1 * 140) / 228 = (14 * 140) / 228 = 8.60(N)$

The reaction of the pin support at the point J $R_J = (P_1 * 88) / 228 = (14 * 88) / 228 = 5.40(N)$

To check, the sum of the forces about the y axis is zero: $\Sigma F_y = 0$: $R_J - P_1 + R_F = 5.40 * 1 - 14 + 8.60 * 1 = 0$

Considering the first span of the beam $0 \leq x_1 < 140$, the bending moment M is $M(x_1) = R_J * (x_1)$

The values of M at the edges is

$$M_1(0) = 5.40 * (0) = 0 (N * mm)$$

$$M_1(140) = 5.40 * (140) = 756.49 (N * mm)$$

For the second span of the beam $140 \leq x_2 < 228$ we have $M(x_2) = R_J * (x_2) - P_1 * (x_2 - 140)$

The values of M at the edges of the span:

$$M_2(140) = 5.40 \cdot (140) - 14 \cdot (140 - 140) = 756.49 \text{ (N} \cdot \text{mm)}$$

$$M_2(228) = 5.40 \cdot (228) - 14 \cdot (228 - 140) = 0 \text{ (N} \cdot \text{mm)}$$

The maximum bending stress is given by

$$\sigma = \frac{MC}{I}$$

In which:

M=the internal bending moment about the section's neutral axis, calculated above as 756.49 (N.mm).

c=the perpendicular distance from the neutral axis to the farthest point on the section, approximately 5mm.

I=the moment of inertia of the section area about the neutral axis. The second moment of the area at the maximum M is $I=85 \text{ mm}^4$

So

$$\sigma_{\max} = \frac{756.5 \times 5}{85} = 45 \text{ [N} \cdot \text{mm}^{-2}]$$

Note that yield strengths for Ductile Iron typically is 275 MPa. Therefore the safety factor is obtained as

$$n = \frac{\sigma_{\text{Yield}}}{\sigma_{\max}} = \frac{275}{45} = 6$$

The values measured based on the worst-case shows the legs stand the exerted forces. Figure 16 shows the moment and shear diagrams.

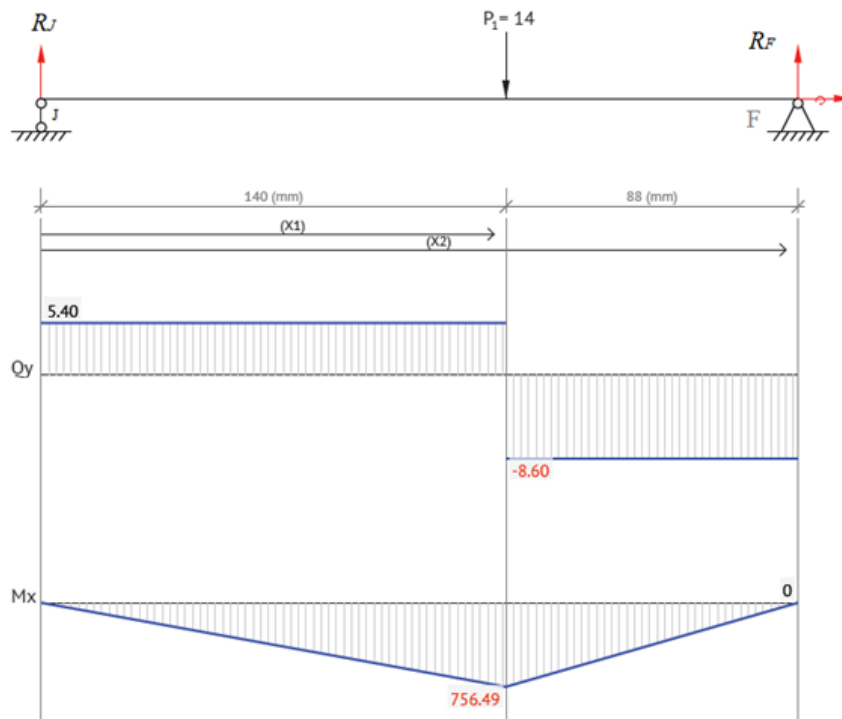


Fig 16. Evaluation of the mechanical strength.

6 Simulations vs Experimental Work

In order to obtain numerical values, the driver link is supposed to be rotating with a constant angular velocity of 15 RPM provided by a velocity controlled motor. Figure 17 shows the results for the robot velocity and acceleration. The values show the

ideal case, while the experiment may depend on the ground specifications including friction and hardness effects. Note that at $t=2$ s there is a discontinuity due to the collision of the feet and switching steps. The research was followed by the fabrication of the actual system shown in Figure 18.

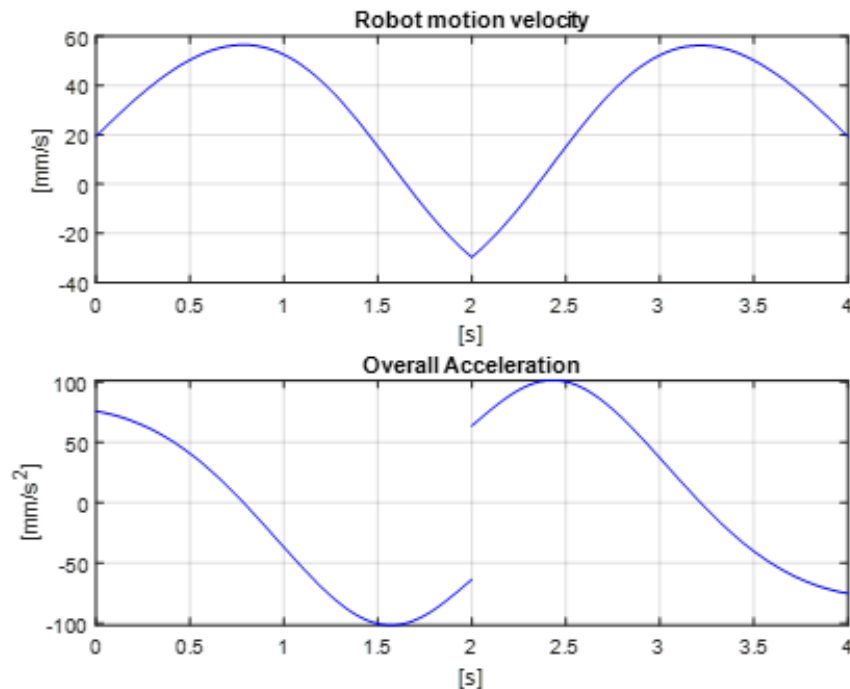


Fig 17. The gross motion velocity and acceleration.

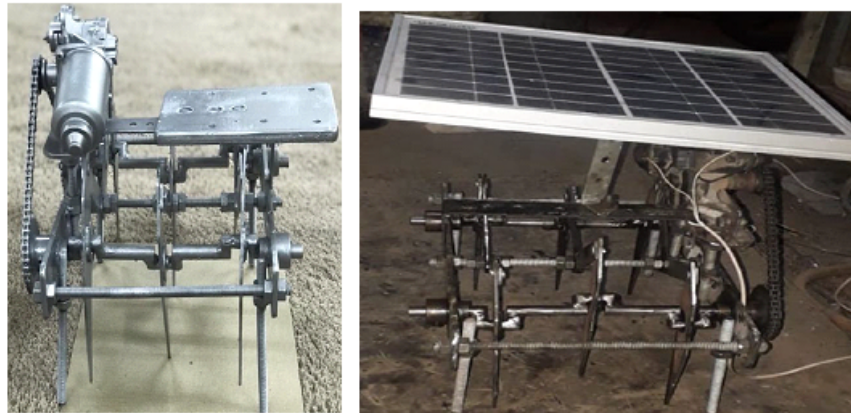


Fig 18. The fabricated prototype of the hexapod walker with a solar panel for future studies (right).

The dynamic equation of the system during walking is not presented in this paper, as a model-based controller has not been planned. The equations may be described by the motion equations as well as impact mechanics for the interaction of the feet with the ground. The dynamic equations are achieved by deriving the governing equations of motion for the mechanism. Well-known methodologies are Newton-Euler and Euler-Lagrange method. The Newton-Euler method is based on the vector approach and consists of three translation equations and three rotation equations for each link. The equations are combined with constraint equations of the joints and loop closure. The Euler-Lagrange equation is generally written in the matrix form

of:

$$M(\theta) + C(\theta, \dot{\theta}) + G(\theta) = T$$

As an approximation, the overall mass of the stationary parts can be supposed at point O, and half of the mass of each link can be considered as lumped masses at the ends of the links. The following masses can be defined

M_{JL1}	Lumped mass at point JL1	$0.5 \times \text{Mass of upper arm} + 0.5 \times \text{Mass of forearm}$
M_{AL1}	Lumped mass at point AL1	$0.5 \times \text{Mass of driver link}$
M_{FL1}	Lumped mass at point FL1	$0.5 \times \text{Mass of forearm}$
M_O	Lumped mass at point O	$\text{Mass of fixed parts} + 0.5 \times \text{Mass of upper arms and drivers}$

As L1 and L3 legs move together, one can combine the mass of L3 in L1 (likewise R3 in R1). A lumped inertia I_o is considered to include inertial effects. The numerical values are as follows:

$$M_O = 2.600, M_{J1} = 0.2, M_{AL1} = 0.05, M_{FL1} = 0.2, \\ I_O = 0.1, M_{J2} = 0.1, M_{AL1} = 0.05, M_{FL2} = 0.1$$

Figures 19 and 20 show the approximated value of the required torque to provide a 15 RPM speed for the driver link. Note that the diameters of the pulleys are supposed to be equal for all of the pulleys. With a speed controlled servomotor, the dynamics is treated as perturbations which are rejected by the built-in automatic feedback control of the servomotor.

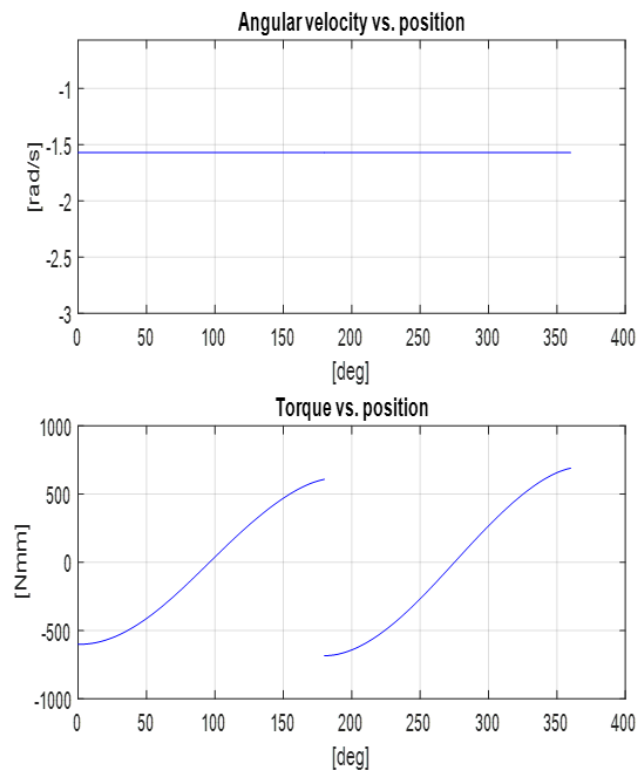


Fig 19. Motion and torque of the driver link.

Dynamic effects are generally ignored at low speeds. With the solar panel, the robot can be used in remote lands, where short and occasional repositioning is required. Further investigations are in progress to use the robot in the real environment, various surfaces, etc.

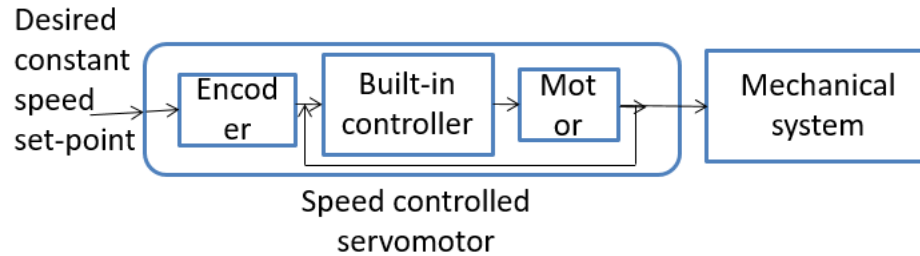


Fig 20. The required torque and the control block diagram.

7 Conclusions

The main focus of this paper was on the kinematics of a single actuator hexapod robot. A six-legged robot was designed and fabricated based on crank rocker mechanisms. The overall dimensions of the mechanism were selected so that the crank rocker function is ensured. Then, the six-legged robot was designed with connecting six of the mechanisms. The kinematic equations were derived using vector analysis and hypothesis on the boundary conditions representing the ground interaction with the feet. The robot gait analysis was performed with the velocity analysis and simulations, and the overall motion of the robot was presented. The simulation results showed that the robot was able to walk based on the described gait. The robot was fabricated and tested successfully. The robot is proposed for moving in remote environments where low-speed repositioning is required. As future work, it is suggested that the gait should be investigated experimentally for various surfaces with different friction properties.

References

- 1) Bhandari VB. Design of Machine Elements. In: and others, editor. Tata McGraw-Hill Education. 2017;p. 944–944.
- 2) Acary V, Brogliato B. Numerical Methods for Nonsmooth Dynamical Systems - Applications in Mechanics and Electronics. Berlin Heidelberg. Springer-Verlag. 2008;p. 525–525.
- 3) Al-Bender F, Lampaert V, Swevers J. The generalized Maxwell-slip model: a novel model for friction Simulation and compensation. *IEEE Transactions on Automatic Control*. 2005;50(11):1883–1887. doi:10.1109/tac.2005.858676.
- 4) Al-Bender F, Symens W, Swevers J, Brussel HV. Theoretical analysis of the dynamic behavior of hysteresis elements in mechanical systems. *International Journal of Non-Linear Mechanics*. 2004;39(10):1721–1735. doi:10.1016/j.ijnonlinmec.2004.04.005.
- 5) Mehdigholi H, Akbarnejad S. Optimization of Watt's Six-Bar Linkage to Generate Straight and Parallel Leg Motion. *International Journal of Advanced Robotic Systems*. 2012;9(1):22–22. doi:10.5772/50917.
- 6) Baykus B, Anli E, Ozkol I. Design and Kinematics Analysis of a Parallel Mechanism to be Utilized as a Luggage Door by an Analogy to a Four – Bar Mechanism. *Engineering*. 2011;03(04):411–421. doi:10.4236/eng.2011.34047.
- 7) R MAK, Design. Synthesis And Simulation Of Four Bar Mechanism For Eliminate The Plowing Depth Fluctuations In Tractors. *International Journal of Engineering Research and Applications (IJERA)*. 2013;3:953–956.
- 8) Abdulkadar M, Deshmukh B. Simulation of Four Bar Mechanism For Path Generation. *International Journal of Emerging Technology and Advanced Engineering*. 2013;3:637–640.
- 9) Vanitha U, Premalatha V, Nithinkumar M. Mechanical Spider Using Klann Mechanism. *Scholars Journal of Engineering and Technology (SJET)*. 2015;3:737–740.
- 10) Arinjay PS, Khot VJ. Design of Bio-Mimic Hexapod. *IOSR Journal of Mechanical and Civil Engineering*. 2013;10:14–20.
- 11) Nelson GM. Learning about control of legged locomotion using a hexapod robot with compliant pneumatic actuators. Cleveland, Ohio, USA. 2002.
- 12) Tanaka G, Takamura T, Shimura Y, IEEE, et al. Development of Simulator and Analysis of Walking for Hexapod Robots. In: and others, editor. 58th Annual Conference of the Society of Instrument and Control Engineers of Japan (SICE). IEEE. 2019;p. 1594–1599.
- 13) Roy SS, Singh AK, Pratihari DK. Analysis of Six-legged Walking Robots. In: and others, editor. 14th National Conference on Machines and Mechanisms (NaCoMM09), NIT, Durgapur, India. 2009;p. 259–265.
- 14) Deepak D, Pathmasharma S. Design and Fabrication of Kinematic Robotic Walker with Left and Right Motion with Camera. *SSRG International Journal of Mechanical Engineering*. 2017;4:53–56.
- 15) Bombléd Q, Verlinden O. Current Sensing in a Six-Legged Robot. In: G S, LL K, A T, editors. IUTAM Symposium on Dynamics Modeling and Interaction Control in Virtual and Real Environments. Dordrecht. Springer. 2011;p. 73–80.
- 16) Singh R, Bera TK. Walking Model of Jansen Mechanism-Based Quadruped Robot and Application to Obstacle Avoidance. *Arabian Journal for Science and Engineering*. 2020;45(2):653–664. doi:10.1007/s13369-019-04135-8.
- 17) Garcia E, Arevalo JC, Munoz G. On the biomimetic design of agile-robot legs. *Sensors*. 2011;11:11305–11334.
- 18) Grzelczyk D, Szymanowska O, Awrejcewicz J. Kinematic and dynamic simulation of an octopod robot controlled by different central pattern generators. *Proceedings of the Institution of Mechanical Engineers, Part I: Journal of Systems and Control Engineering*. 2019;233(4):400–417. doi:10.1177/0959651818800187.

- 19) Leng X, Piao S, Chang L, He Z, Zhu Z. Dynamic running hexapod robot based on high-performance computing. *The Journal of Supercomputing*. 2020;76(2):844–857. doi:10.1007/s11227-019-02988-2.
- 20) Gao H, Liu Y, Ding L. Low Impact Force and Energy Consumption Motion Planning for Hexapod Robot with Passive Compliant Ankles. *Journal of Intelligent & Robotic Systems*. 2019;94:349–370.
- 21) Bai L, Hu H, Chen X. CPG-Based Gait Generation of the Curved-Leg Hexapod Robot with Smooth Gait Transition. *Sensors*. 2019;19:3705–3705.
- 22) Wang G, Ding L, Gao H, et al. Minimizing the Energy Consumption for a Hexapod Robot Based on Optimal Force Distribution. *IEEE Access*. 2019.
- 23) Zhou X, Wei W, Gao Y. Research on Terrain Recognition for Gait Selection of Hexapod Robot. *IOP Conference Series: Materials Science and Engineering*. 2019;p. 12072.
- 24) Yang JM. Fault-Tolerant Gait Planning for a Hexapod Robot Walking over Rough Terrain. *Journal of Intelligent and Robotic Systems*. 2009;54:613–627.
- 25) Dürr V, Arena PP, Cruse H. Integrative biomimetics of autonomous hexapedal locomotion. *Frontiers in neurorobotics*. 2019;13.
- 26) Saranlı U, Buehler M, Koditschek DE. RHex: A Simple and Highly Mobile Hexapod Robot. *The International Journal of Robotics Research*. 2001;20(7):616–631. doi:10.1177/02783640122067570.
- 27) Tedeschi F, Carbone G. Design Issues for Hexapod Walking Robots. *Robotics*. 2014;3(2):181–206. doi:10.3390/robotics3020181.
- 28) Desai SG, Annigeri AR, TimmanaGouda A. Analysis of a new single degree-of-freedom eight link leg mechanism for walking machine. *Mechanism and Machine Theory*. 2019;140:747–764. doi:10.1016/j.mechmachtheory.2019.06.002.
- 29) Zang H, Zhao D, Shen L. Multi-Legged Robot Based on Single Continuous Driving Bionic Leg. *International Journal of Robotics and Automation*. 2019;34(6). doi:10.2316/j.2019.206-0058.
- 30) Mikami S, Fukuda T. Mechanical and Gait Design for Roll-Free Multiple Legged Robot Driven by Single Motor. In: and others, editor. 2017 First IEEE International Conference on Robotic Computing (IRC). IEEE. 2017;p. 143–147.
- 31) Marghitu DB. Springer Science & Business Media. 2009.